DOI: 10.1002/cbic.200500218

Quantum-Dot Aptamer Beacons for the Detection of Proteins

Matthew Levy, Sean F. Cater, and Andrew D. Ellington*[a]

Quantum dots (QDs) offer a number of advantages over standard fluorescent dyes for monitoring biological systems in real time, including greater photostability, larger effective Stokes shifts, longer fluorescent lifetimes, and sharper emission bands than traditional organic fluorophores. In addition, QDs all respond to the same excitation wavelength, but emit at different wavelengths; this should allow for the multiplex detection of different analytes in parallel.

Recent work has also demonstrated that QDs can be used in the construction of biosensors that signal by fluorescence resonance energy transfer (FRET). For example, a quantum-dot-based molecular beacon has been described in which the non-fluorescent dye DABCYL was used to quench the fluorescence of the quantum dot. In the presence of a target DNA, the opening of the molecular beacon resulted in an approximately fivefold increase in fluorescence of the quantum dot.[1] Similarly, a QD-based protein biosensor that can detect the small molecule maltose has been designed. In one configuration of this system, a maltose-binding protein was complexed to the ZnS shell of a CdSe QD through a 5-histidine tail appended to the protein. Binding of a dye-labeled cyclodextrin molecule to the protein resulted in a loss of photoluminescence, which could be restored by the displacement of the bound cyclodextrin by the addition of maltose.[2]

We have now designed a quantum-dot-based aptamer biosensor. Like molecular beacons, aptamer beacons rely on analyte-dependent conformational changes that can alter the proximity of optical reporters to one another, and thus can potentially alter the fluorescence resonance energy transfer (FRET) between these reporters. Aptamer beacons have previously been designed for a variety of targets including small molecules, such as ATP and cocaine, and protein targets, such as PDGF, thrombin, and the HIV-1 Tat.[3–9]

We utilized an aptamer that is known to bind the blood-clotting protein thrombin as a model system.[10] While thrombin aptamer beacons that utilize organic fluorophores have previously been developed,[5–7] the adaptation of these strategies to the development of a quantum-dot aptamer beacon (QDB) was not straightforward, primarily because the inorganic quantum dot is much larger and brighter than its organic partner. The development of quantum-dot beacons therefore relied upon two important design features.

First, in order to ensure that a substantive conformational change would occur upon analyte binding, we synthesized a quantum-dot beacon based on a two-piece aptamer beacon originally developed by Li et al. in 2002. The final construct consisted of the anti-thrombin aptamer conjugated to a quantum dot (Figure 1A; underlined), and an oligonucleotide

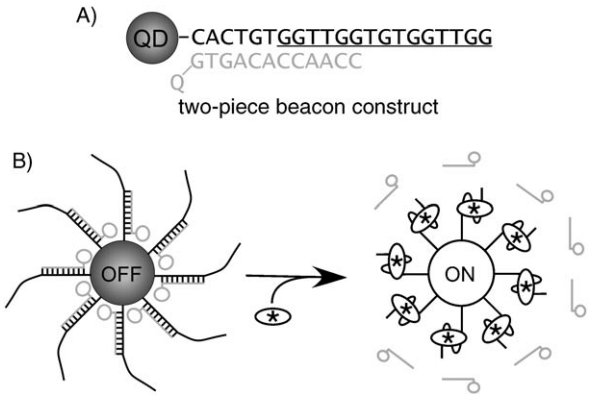

Figure 1. Design of a quantum-dot aptamer beacon for the detection of thrombin. A) Sequence of anti-thrombin aptamer (black) and quench oligonucleotide (gray). The portion of the anti-thrombin aptamer known to form a quadruplex has been underlined. B) Schematic for detection. Binding of target (*) stabilizes the displacement of the quench oligonucleotide (gray) and enhances the fluorescence of the quantum dot. Since the quantum dots have multiple streptavidin molecules on their surfaces, multiple aptamers are associated with a single quantum dot.

quencher conjugate that hybridized to and disrupted the aptamer structure (Figure 1A; gray). In the presence of the target protein, thrombin, the quadruplex conformation of the aptamer should be preferentially stabilized, resulting in the displacement of the antisense oligonucleotide quencher conjugate and a concomitant increase in fluorescence (Figure 1B).

Second, to ensure that the quantum dot was efficiently quenched, multiple aptamer beacon–oligonucleotide quencher pairs were immobilized on each QD. Quenching is generally less efficient with quantum dots than with organic fluorophores because of the distance limitations imposed by the quantum-dot shell and the coatings required for water solubility. Multiple quenchers have previously proven useful in overcoming these distance limitations.[2,11]

The relationship between the efficiency of quenching (E) and the number of quencher molecules is given by Equation (1):

$$E = \frac{nR_0^6}{nR_0^6 + r^6} \quad (1)$$

Here n is the number of quencher molecules, R_0 is the Förster radius, and r is the separation distance. In the case of the streptavidin-coated Qdot525 (Qdot Corporation, Haywood, CA) used in these studies, the reported diameter is ~15 nm; this places the dye molecules ~75 Å from the core. Because efficient quenching also relies on good spectral overlap between the quencher and the QD fluorescence emission, we chose to use the Eclipse quencher (Glen Research, Sterling, VA), which

[a] M. Levy, S. F. Cater, Prof. A. D. Ellington
Institute for Cellular and Molecular Biology, University of Texas, Austin
Austin TX, 78712 (USA)
Fax: (+1) 512-471-7014
E-mail: andy.ellington@mail.utexas.edu

has a reported λ_{max} of 530 nm and thus should provide an excellent overlap with the streptavidin-coated Qdot525.

The Förster radius for the Eclipse dye–QD FRET pair can be calculated from Equation (2):

$$R_0 = 0.211[\kappa^2 n^4 Q_D J]^{1/6} \quad (2)$$

Here κ is the orientation factor ($\kappa^2 = {}^2/_3$ for random collisions), n is the index of refraction in aqueous solution ($n \approx 1.33$), Q_D is the quantum yield of the QDs (~40%), and J is the overlap integral for the dye and the QD. Overlap integrals were in turn calculated from Equation (3):

$$J = \frac{\int_0^\infty F_D(\lambda)\varepsilon_A(\lambda)\lambda^4 d\lambda}{\int_0^\infty F_D(\lambda) d\lambda} \quad (3)$$

Here F_D is the normalized emission spectra of the donor and ε_A is the molar extinction coefficient of the acceptor.

In the case of our aptamer construct, the absorbance spectrum for the Eclipse quencher was experimentally measured by using a singly labeled quench oligonucleotide (Q1; Figure 2; squares). The maximum emission was found to be slightly longer ($\lambda^{Q1}_{max} = 541$ nm, $\varepsilon^{Q1}_{max} = 33\,000$) than the reported value. To help ensure efficient quenching, we also synthesized a second quench oligonucleotide bearing two Eclipse quenchers (Q2; Figure 2; circles). The maximum emission of this construct was experimentally found to be slightly shorter than expected ($\lambda^{Q2}_{max} = 522$ nm, ε^{Q2}_{max} estimated as 66 000). Nonetheless, both quench oligonucleotides showed an excellent spectral overlap with the fluorescence emission of the QD (Figure 2). Based on these equations, we estimated that it would require ~40 Q1 oligonucleotides or ~20 Q2 oligonucleotides to quench the fluorescence of the QDs by ~80%.

The level of quenching was determined empirically by a titration experiment in which streptavidin-coated quantum dots (2.5 nM) were incubated with increasing amounts of the biotinylated aptamer oligonucleotide bound by quench oligonucleotides. The oligonucleotides were mixed and thermally equilibrated in signaling buffer (20 mM Tris-HCl pH 8.2, 5 mM KCl, 1 mM $MgCl_2$) prior to the addition of the quantum dots. After mixing, the solutions were incubated for 60 min, and the resultant fluorescence was measured by using a Tecan Safire fluorescence microtitre plate reader. Fluorescence emission was measured from 460 nm to 600 nm at a fixed excitation wavelength of 400 ± 12.5 nm. A plot of the relative fluorescence at the emission max versus the number of biotinylated oligonucleotides per quantum dot (Figure 3) indicates that saturation of streptavidin-binding sites on the quantum-dot surface occurs at ~40 biotinylated oligonucleotides per dot with an ultimate quenching efficiency of ~75% for quench oligonucleotide Q1 and ~95% for Q2. These experimental values compare very well with the values calculated from Equation (1)—the predicted levels of quenching are shown as lines in Figure 3. Similar experiments conducted with a quench oligonucleotide that contained four Eclipse quenchers resulted in nonspecific quenching, even in the absence of the biotinylated aptamer oligonucleotide (data not shown).

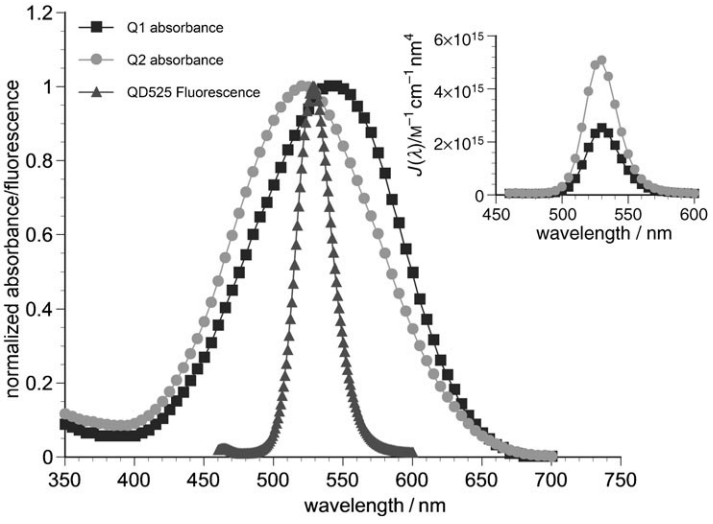

Figure 2. Normalized fluorescence and absorbance of the quantum dot and quench oligonucleotides Q1 and Q2 used in these studies. Inset: the overlap integral $J(\lambda)$ for the interaction was calculated as described in the text. For the QD:Q1 overlap, this gives $J(\lambda) = 2.5 \times 10^{15}\,\text{M}^{-1}\text{cm}^{-1}\text{nm}^4$ and for QD:Q2 this gives $J(\lambda) = 4.9 \times 10^{15}\,\text{M}^{-1}\text{cm}^{-1}\text{nm}^4$.

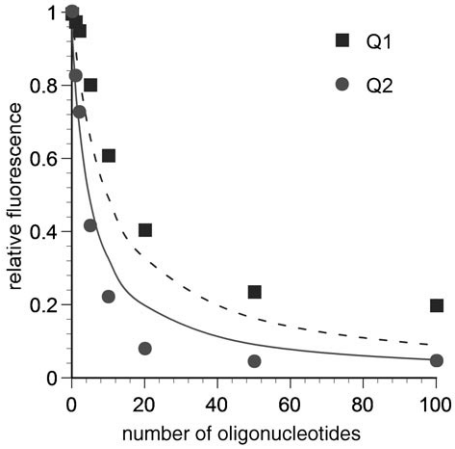

Figure 3. Loss of quantum-dot fluorescence with increasing number of quench oligonucleotides. The dashed line represents the values calculated from Equation (1) for Q1, while the solid line represents the values for Q2.

Using Q2 and optimal quenching conditions, we conducted experiments to determine if the QDB construct could be activated by a complementary oligonucleotide. Two different complementary oligonucleotides were synthesized for this purpose (Figure 4). Comp. **1** is perfectly complementary to the biotinylated aptamer oligonucleotide shown in Figure 1A, while Comp.m**1** contains a two-base-pair internal mismatch (boxed residues). As shown in Figure 4, when reactions were carried out at 37 °C, the addition of a tenfold excess of Comp.**1** to a thermally equilibrated mixture of streptavidin-coated quantum dots conjugated to Q2 and biotinylated aptamer (corresponding to a 1:2:10 aptamer/Q2/target ratio) resulted in a steady increase of fluores-

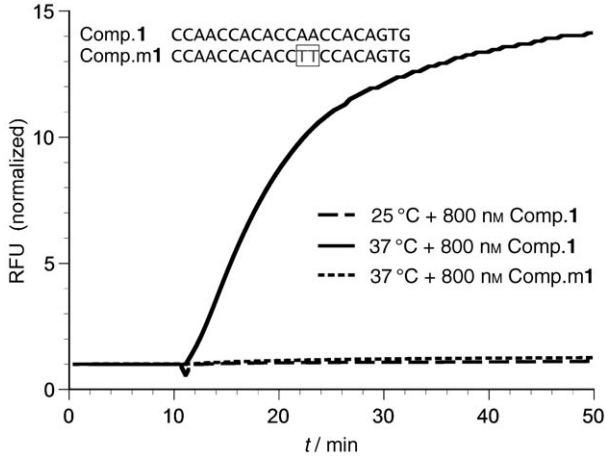

Figure 4. Real-time detection of an oligonucleotide target. Complementary or mismatched oligonucleotides were added at $t = 10$ min. The increase in fluorescence was only observed in the presence of the complementary nucleic acid target at 37 °C. The lack of activation at 25 °C is consistent with the slow rate of strand displacement and exchange at this temperature.

cence. Addition of the double mutant Comp.m**1** had no effect on fluorescence intensity. Reactions conducted with Comp.**1** at 25 °C similarly showed no response. The lack of activation at 25 °C is consistent with the fact that the aptamer–Q2 complex is predicted to have a melting temperature of ~40 °C.[12] Overall, the QDB construct showed a 14-fold increase in fluorescence in the presence of the target nucleic acid. This observed increase in fluorescence is comparable to the ~10–60-fold increase commonly observed for molecular beacons containing organic dyes.[13–15]

Finally, we performed a similar set of experiments to detect the protein thrombin. Again, the sample was incubated in the absence of target for 10 min prior to the addition of 1 μM thrombin. As shown in Figure 5, a rapid increase in fluorescence was observed upon the addition of thrombin. No signal increase was observed upon the addition of a nonspecific protein, lysozyme. Overall, the QDB construct showed a 19-fold increase in fluorescence in the presence of the cognate protein target. This observed increase in fluorescence was similar to that observed for a similar construct designed on traditional organic fluorophores (19-fold vs. 12-fold).[6]

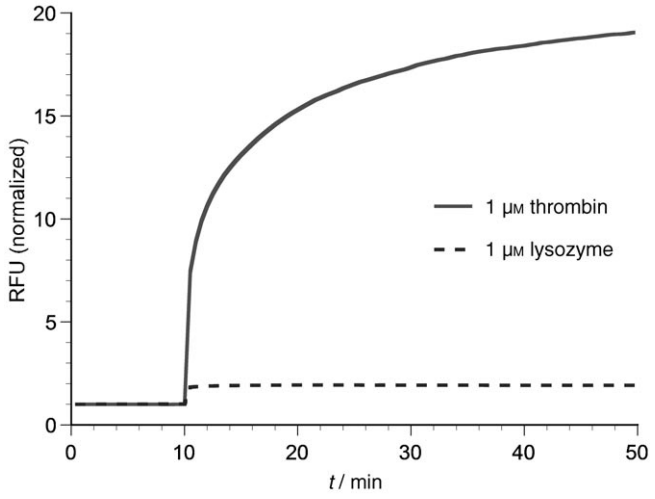

Figure 5. Real time detection of thrombin. Thrombin or the nonspecific target lysozyme was added at $t = 10$ min. Reactions were carried out at 37 °C.

These experiments pave the way for the expansion of QDB detection methods to other targets and analytes. The fact that different QDBs can have finely tuned wavelength emissions should allow multiple different target molecules to be assayed in parallel in heterogeneous solution. By immobilizing different aptamer constructs onto different quantum dots, it should be possible to carry out multiplexed protein detection. As might be expected, in addition to quenching dots that emitted at 525 nM, our QDB construct also quenched quantum dots that emitted at 565 and 585 nm by ~90% and even quenched dots that emitted at 605 nm by ~60% (data not shown). It is likely that additional quantum dots with nonoverlapping emission spectra and additional quenchers that efficiently work at wavelengths longer than 600 nm can be used to further increase the number of analytes that can be assayed in parallel.

Experimental Section

All oligonucleotides were synthesized on an Expidite 8909 DNA synthesizer (PE Biosystems, Foster City, CA) by using standard phosphoramidite chemistry. All synthesis reagents were purchased from Glen Research (Sterling, VA). The 3′ Eclipse-bearing oligonucleotides were synthesized by starting from Eclipse-CPG. Multiple Eclipse dyes were added by using the Eclipse phosphoramidite. The 5′ biotin was added during solid-phase synthesis by using a 5′ biotin phosphoramidite. All oligonucleotides were purified on either 15% (aptamer constructs) or 20% (quench oligonucleotides) denaturing (7 M urea) polyacrylamide gels. The sequence of the biotinylated anti-thrombin aptamer was 5′B-TTCACTGTGGTTGGTGTGGTTGG, in which B is a 5′ biotin. The sequence of quench oligonucleotide Q1 was 5′-CCAACCACAGTG-Q, and that of oligonucleotide Q2 was 5′-CCAACCACAGTG-Q-Q, where Q is the Eclipse quencher. Oligonucleotide concentrations were quantitated by UV absorbance at 260 nm on a NanoDrop ND-1000 spectrophotometer (NanoDrop Technologies, Wilmington, DE). UV-visible absorbance spectra were recoded on a Shimadzu UV-1601 spectrophotometer (Shimadzu Corporation, Columbia, MD).

Qdot525–streptavidin conjugates (lot number 0304–0059) were purchased from the Qdot Corporation (Hayward, CA). The quantum-dot emission spectra were measured from 460 to 600 nm by using a PTI fluorometer with an excitation wavelength of 400 ± 20 nm (Photon Technology International, Lawrenceville, NJ).

Oligonucleotide activation assays were conducted as follows. A mixture of quench oligonucleotide Q2 (1.6 μM) and biotinylated aptamer (800 nM) was thermally equilibrated in signaling buffer (20 mM Tris pH 8.2, 5 mM KCl, 1 mM $MgCl_2$) by heating it to 70 °C for 3 min, then cooling it to room temperature. The solution was subsequently diluted twofold and incubated with streptavidin-coated quantum dots (20 nM) for 1 h at room temperature in signaling buffer. Reactions were diluted tenfold to a final volume of 250 μL prior to analysis. The final concentrations of reagents were 2 nM quantum dots, 40 nM biotinylated aptamer, and 80 nM oligonucleo-

tide Q2. The fluorescence was determined to be stable over a 10 min period, then the oligonucleotide target (800 nM, 2.5 μL at 80 μM) was added, and fluorescence was recorded for another 50 min. All assays were monitored in real time at 525 nm with a PTI fluorometer at an excitation wavelength of 400 ± 20 nm. Time points were recorded every 30 s.

Thrombin activation assays were conducted in a manner similar to the oligonucleotide activation assays described above. Reactions were carried out at 37 °C. Thrombin (Sigma, St Louis, Mo) and the nonspecific control protein lysozyme (Sigma, St Louis, MO) were added to a final concentration of 1 μM (2.5 μL at 100 μM).

Keywords: aptamer beacons · nucleic acids · proteins · quantum dots · signaling aptamers

[1] J. H. Kim, D. Morikis, M. Ozkan, *Sens. Actuators B* **2004**, *102*, 315 – 319.
[2] I. L. Medintz, A. R. Clapp, H. Mattoussi, E. R. Goldman, B. Fisher, J. M. Mauro, *Nat. Mater.* **2003**, *2*, 630 – 638.
[3] R. Yamamoto, T. Baba, P. K. Kumar, *Genes Cells* **2000**, *5*, 389 – 396.
[4] X. Fang, A. Sen, M. Vicens, W. Tan, *ChemBioChem* **2003**, *4*, 829 – 834.
[5] N. Hamaguchi, A. Ellington, M. Stanton, *Anal. Biochem.* **2001**, *294*, 126 – 131.
[6] R. Nutiu, Y. Li, *J. Am. Chem. Soc.* **2003**, *125*, 4771 – 4778.
[7] J. J. Li, X. Fang, W. Tan, *Biochem. Biophys. Res. Commun.* **2002**, *292*, 31 – 40.
[8] M. N. Stojanovic, P. de Prada, D. W. Landry, *J. Am. Chem. Soc.* **2001**, *123*, 4928 – 4931.
[9] M. N. Stojanovic, P. de Prada, D. W. Landry, *J. Am. Chem. Soc.* **2000**, *122*, 11 547 – 11 548.
[10] L. C. Bock, L. C. Griffin, J. A. Latham, E. H. Vermaas, J. J. Toole, *Nature* **1992**, *355*, 564 – 566.
[11] A. R. Clapp, I. L. Medintz, J. M. Mauro, B. R. Fisher, M. G. Bawendi, H. Mattoussi, *J. Am. Chem. Soc.* **2004**, *126*, 301 – 310.
[12] R. Owczarzy, Y. You, B. G. Moreira, J. A. Manthey, L. Huang, M. A. Behlke, J. A. Walder, *Biochemistry* **2004**, *43*, 3537 – 3554.
[13] S. Tyagi, F. R. Kramer, *Nat. Biotechnol.* **1996**, *14*, 303 – 308.
[14] W. Tan, X. Fang, J. Li, X. Liu, *Chem. Eur. J.* **2000**, *6*, 1107 – 1111.
[15] D. L. Sokol, X. Zhang, P. Lu, A. M. Gewirtz, *Proc. Natl. Acad. Sci. USA* **1998**, *95*, 11 538 – 11 543.

Received: May 24, 2005
Published online on October 27, 2005

